Sustainable Food Technology

ROYAL SOCIETY OF CHEMISTRY

PAPER

View Article Online
View Journal | View Issue

Cite this: *Sustainable Food Technol.*, 2025, **3**, 1035

Fabrication and characterization of methylcellulose/chitosan active films incorporated with L-arginine and their potential in the green packaging of grapes

Suhasini Madihalli,[a] Saraswati P. Masti, *[a] Manjunath P. Eelager,[a] Manjushree Nagaraj Gunaki,[a] Ravindra B. Chougale,[b] Nagarjuna Prakash Dalbanjan[c] and S. K. Praveen Kumar [c]

Active biodegradable films are in great demand as green packaging materials for extending the shelf life of food. In this study, methylcellulose (MC)/chitosan (CS) active films (AMC) were fabricated by incorporating different weight percentages of L-arginine. The fabricated active films were investigated for their physicochemical, mechanical and functional properties. FTIR, SEM and XRD results confirmed the intermolecular hydrogen bonding interaction and compatibility of L-arginine with the MC/CS film matrix, improving the mechanical properties, UV light blocking ability, water vapor barrier and oxygen barrier properties of the AMC active films. The inclusion of L-arginine improved the antimicrobial, antioxidant and packaging efficiency of the films. Compared with the L-arginine-free MC/CS film (control), the AMC active film containing 7.5% of L-arginine exhibited strong DPPH radical scavenging activity (72.28% ± 0.28) and displayed potent antimicrobial activity against *E. coli*, *S. aureus*, *B. subtilis* and *C. albicans*. Grapes packed with the AMC active film containing 7.5% L-arginine showed a limited weight loss percentage of 13.35% ± 1.07 and a restricted browning degree of 0.87 ± 0.01 over 17 days of storage. These findings suggest that the fabricated active films meet the essential prerequisites of green food packaging materials.

Received 30th November 2024
Accepted 29th April 2025

DOI: 10.1039/d4fb00359d

rsc.li/susfoodtech

Sustainability spotlight

The significance of the present study lies in its multifaceted contribution to sustainable and biodegradable food packaging applications. This study addresses the growing concern of environmental problems resulting from synthetic food packaging materials by utilizing L-arginine and natural polysaccharides like methylcellulose and chitosan, offering possibilities for significant advancements in the food packaging sector. The prepared active films exhibited excellent mechanical, water vapor barrier, UV barrier, antibacterial, antioxidant, and biodegradable properties. Furthermore, the active films extended the shelf life of grapes to over 17 days of storage. Hence, these fabricated bioactive films have the potential to reduce food waste while supporting eco-friendly practices, making a valuable contribution to sustainable food packaging.

1. Introduction

Plastics are the most adaptable components of everyday life owing to their ease of processing, resilience, and performance.[1] However, these plastics end up in landfills or get incinerated after their use and remain in the environment for a long time. The extensive use of plastics has negatively impacted the ecosystem and endangered life. They are also proven for their bioaccumulation and biomagnification in the tissues of organisms owing to their resistance to degradation, which has caused microplastics to become an intrinsic component of our food chain with increasing production. It has been reported that this plastic waste also facilitates the colonization of toxin-producing microorganisms by providing a bioadhesion substratum for these microbes, which are detrimental to pelagic and human life.[2] Globally, over 340 million tonnes of plastic waste are generated, with the packaging sector accounting for 46% of the total plastic waste. To address these problems, current research and scientific progress have been promoting bio-based food packaging materials, which can be converted into CO_2, H_2O and biomass within six months after their end use.[3] This strategy is emerging as a sustainable option, especially for short-term applications such as food packaging.[4]

[a]*Department of Chemistry, Karnatak Science College, Dharwad-580 001, Karnataka, India. E-mail: dr.saraswatimasti@yahoo.com*
[b]*P.G. Department of Studies in Chemistry, Karnatak University, Dharwad-580 003, Karnataka, India*
[c]*P.G. Department of Biochemistry, Karnatak University, Dharwad-580 003, Karnataka, India*

Food packaging is crucial in the food supply chain and safety as it is a protective layer that can inhibit unfavorable biological and chemical changes. As a result, packaging materials should serve as a barrier to moisture, oxygen, dust, and chemicals. It should also inhibit the growth of harmful bacteria, odor-causing fungi and other microorganisms that cause food-borne diseases to maintain food quality over a long period.[5–7] Foodborne diseases and bacterial contamination are significant concerns for the food industry. Many physical and chemical processing methods have been used to control these bacterial contaminations. Physical processing methods like thermal inactivation, high-pressure processing and UV treatments can lead to nutrient loss and changes in the appearance of food which reduces its overall quality. Additionally, some chemical preservatives have been used in the food industry. However, their use has failed to meet consumer demands due to their unpleasant taste and potential health problems. It has been reported that various countries have banned the use of some food preservatives, such as boric acid, tartrazine, sunset yellow (azodye) and amaranth (trisodium salt), due to their toxicity and potential carcinogenicity.[8] Thus, in response to modern consumer demands, such as nutritional and safety requirements for food, biopolymers have been extensively used in the development of active food packaging materials.[9–11] Bioactive packaging films incorporated with active components, such as antimicrobial agents and antioxidants, can prolong the food shelf life by inhibiting bacterial activity and maintaining the quality of food products.[12,13] Several biopolymers have been used for fabricating biodegradable packaging materials, such as chitosan,[14] pullulan,[15] cellulose and cellulose derivatives,[16] gelatin,[17] gums, carrageenan,[18] and starch. Chitosan and cellulose derivatives are often employed for fabricating food packaging films due to their attractive properties, such as biodegradability, biocompatibility, abundance and non-toxicity.[19]

Methylcellulose (MC) is the most promising hydrocolloid polysaccharide, comprising (1–4) glycosidic chains with methyl groups. MC is derived from cellulose *via* the partial substitution of the hydroxyl group with methyl substituents. It affords films with potent lipid and oxygen barrier features. Because of its abundance, easy processability, excellent film-forming ability, thermal gelation capability and high strength, it has the potential to be employed as a packaging material.[18,19] However, most biopolymers, including methylcellulose, are susceptible to atmospheric conditions due to their higher water affinity and poor barrier properties.[20] Thus, in the current study, these limitations were overcome by blending MC with chitosan, which imparts a slightly antimicrobial property owing to the action of chitosan.

Chitosan (CS) is a cationic polysaccharide comprising (1–4)-2-amino-2-deoxy-D-glucan, and is an alkaline deacetylated chitin product. In addition to its inherent antimicrobial and antifungal properties, it has demonstrated biocompatible, biodegradable and non-toxic characteristics. Considering these properties, chitosan is used as a packaging material to preserve various food products.[14,21]

Furthermore, active components that inhibit oxidation and microbial growth are incorporated into the polymer matrix to improve its functional properties. L-arginine is one such active component that imparts both of these properties. It is an essential amino acid in plants, and is vital for developmental and cellular activities. It is crucial in minimizing inhibition driven by plant exposure to stress conditions. It significantly prevents the browning of fruits and vegetables by suppressing the oxidation of polyphenols found within them.[22] L-arginine was also reported to maintain the quality of mango fruits by imparting antioxidant properties.[23] Hence, it was selected as an antimicrobial, antioxidant and antibrowning agent to improve the functional characteristics of the active films.

Polysaccharide-based active films with enhanced functional properties are desirable for food packaging applications. Several studies have been reported on the combination of L-arginine and chitosan. Many researchers evaluated the antibacterial activity of L-arginine-modified chitosan in detail, and reported that L-arginine-modified chitosan has desirable biocompatibility, antibacterial activity and anticoagulant properties.[24,25] These qualities suggest the significant potential of L-arginine as a bioactive component. However, no work has been done on the L-arginine-functionalized MC/CS active films. Hence, in the current study, MC and CS are used as green polymers, and L-arginine is used as an active component to enhance the films' functional properties and packaging efficiency. L-arginine was incorporated into the MC/CS matrix to fabricate the highly efficient antimicrobial, antioxidant and antibrowning novel active films by employing eco-friendly solvent casting techniques for food packaging applications. Fabricated active films were evaluated for their physicochemical and mechanical properties. The influence of L-arginine on functional properties (*e.g.*, antimicrobial, antioxidant and antibrowning activity) was determined. Additionally, fabricated active films were practically applied for grape packaging. The packaged grapes' weight loss and browning degree were also evaluated to check the efficacy of the fabricated active films for use in green packaging applications.

2. Materials and methods

2.1. Materials

Chitosan (MW = 20–100 kDa; degree of deacetylation: 75–85%) and methylcellulose (molecular weight = 454.5 g mol^{-1}) with methoxy substitution between 27.5–31.5% and degree of substitution 1.5–1.9 were procured from the Tokyo Chemical Industry (TCI), Japan. Acetic acid was received from Merck Life Sciences India. L-Arginine, glycerol (99.5% AR) and microbial growth media were obtained from Loba Chemie, Pvt. Ltd, India. Milli-Q water was used throughout the experiment.

2.2. Fabrication of the AMC control and active films

Active films were fabricated by adapting the solvent casting technique. MC and CS solutions were prepared by separately dissolving 1.5 g of MC and 0.5 g of CS in Milli-Q water and 1% acetic acid, respectively. Then, both solutions were blended and

stirred for 6 h to obtain homogeneous blend solutions. Furthermore, 1% (w/v) glycerol was added as a plasticizer. Then, different weight percentage of L-arginine solutions prepared by dissolving the predetermined amounts of L-arginine 0%, 2.5%, 5.0% and 7.5% (w/w of the net dry mass of polymer) in Milli-Q water were added to the blended solutions and stirred for 4 h. The resulting film-forming solutions were cast in Petri plates, and left to dry for 48 h in a hot air oven set to 40 °C. The dried films were peeled off, packed in a zipper storage bag, and stored in a desiccator for further characterization. Films were labeled as AMC-1 (Control), AMC-2, AMC-3 and AMC-4 based on the weight percentages of L-arginine, *i.e.*, 0, 2.5, 5.0 and 7.5%, respectively, before analysis. The MC/CS film without L-arginine was labeled AMC-1 and treated as a control.

2.3. Characterization of the fabricated control and active films

2.3.1. Fourier transform infrared spectroscopy (FTIR). Fourier transform infrared (FTIR) spectra of the fabricated AMC control and active films were recorded using an FTIR spectrometer (Shimadzu Japan) in the 400 to 4000 cm^{-1} frequency range with 4 cm^{-1} sensitivity.

2.3.2. Surface morphology. Surface micrographs of the control and active films were captured using a scanning electron microscope (model JEOL JSM-IT500LA) operating at a 10 kV acceleration voltage. Film samples were coated with a gold layer using a sputtering method before analysis and mounted on a metal stab to capture images.

2.3.3. X-ray diffraction (XRD) analysis. X-ray diffractograms of the fabricated control and active films were recorded using an XRD diffractometer (Rigaku Smart Lab, Tokyo, Japan) with an acceleration of 40 kV. The samples were evaluated using a Cu Kα (λ = 1.5418 Å) filter and 30 mA current at 5° per minute scan range over a 2θ = 5° to 80° angular range. The crystallinity percentage was obtained according to the previously reported method using eqn (1).[26,27]

$$\text{Crystallinity}(\%) = \frac{A_c}{(A_c + A_a)} \times 100 \quad (1)$$

where A_c = area of the crystalline region and A_a = area of the amorphous region.

2.3.4. Film thickness and mechanical properties. The thickness of the fabricated control and active films was measured using a digital micrometer (Mitutoyo, Japan) with 0.001 mm precision. A universal testing machine (Model: UTM, DAK System, 7200-1KN) was employed to measure the mechanical parameters as per ASTM D882-1992. For analysis, 20 × 100 mm film samples were inserted in the extension grip, maintaining a grip separation of 50 mm, and were stretched at a cross-head speed of 1 mm min^{-1} at RT until they fractured.

2.3.5. Surface wettability test. The surface wettability characteristic of the fabricated control and active films was studied using the sessile drop method by employing a contact angle analyzer (Model DMs-401, Kyowa Interface Science Co. Ltd, Tokyo).

2.3.6. Moisture adsorption (MA) and water solubility (WS). Film samples with dimensions of 20 × 20 mm were taken for analysis. The dry mass (m_1) was recorded after heating the samples at 100 °C for 24 h. After that, they were exposed to atmospheric conditions for 24 h and their final mass (m_2) was recorded. The average moisture adsorption values were calculated using eqn (2).[28]

$$\text{Moisture adsorption}(\%) = \frac{m_2 - m_1}{m_2} \times 100 \quad (2)$$

For the water solubility, film samples with dimensions of 20 × 20 mm were taken, and their initial mass (W_1) was noted after dehydrating them at 70 °C for 24 h. The dried samples were soaked in 20 mL of Milli-Q water for 24 h. Then, the undissolved samples were extracted and dried at 70 °C for 24 h to determine their final mass (W_2). The average water solubility values were calculated using eqn (3).[29]

$$\text{Water solubility}(\%) = \frac{W_1 - W_2}{W_1} \times 100 \quad (3)$$

where W_1 = initial weight of the sample and W_2 = final weight of the sample.

2.3.7. UV-visible spectroscopy. A UV-vis spectrophotometer (Model UV-1601) was used to inspect the optical properties of the fabricated AMC control and active films. The film samples with dimensions of 10 × 40 mm taken for the analysis were directly inserted into the test cell, and the spectra were recorded in the wavelength range between 200 and 800 nm using air as a reference. The results were expressed as a percentage of transmittance. Meanwhile, the opacity of the film samples was calculated using eqn (4).[30]

$$\text{Opacity} = \frac{\text{Absorbance}}{\chi} \quad (4)$$

where X = film thickness in mm.

2.3.8. Water vapour transmission rate (WVTR). The WVTR of the fabricated control and active films was determined according to the previously reported method, with some modifications.[31,32] To summarize, film samples with dimensions of 30 × 30 mm were sealed at the circular mouth of glass vials filled with 10 mL of Milli-Q water and fitted with Teflon tape. The initial mass of the glass vials was recorded as W_i, and the weighed samples were maintained in an oven at 40 °C for 24 h. The glass vials were retrieved from the oven and weighed to obtain the final mass (W_f). The transmission rate of the water vapours through the control and active films was then calculated using eqn (5).

$$\text{WVTR} = \left[\frac{W_i - W_f}{A \times T}\right] (\text{g m}^{-2}\ \text{h}^{-1}) \quad (5)$$

where W_i = initial weight of the sample, W_f = final weight of the sample, A = area of the circular mouth of the glass vial, and T = time employed (24 h).

2.3.9. Oxygen permeability (OP). OP was determined according to the previous method, with some alterations.[17] In short, 30 × 30 mm films were secured at the tip of glass vials

and sealed with Teflon tape. Vials were weighed to record their initial weight (W_1) and positioned in a desiccator containing anhydrous $CaCl_2$ at room temperature. After that, the glass vials were taken from the desiccator every 24 h, and their weight was recorded for 3 days. The slopes (g h^{-1}) were calculated using linear regression ($R_2 > 0.982$) and the oxygen permeability (OP) was determined by applying eqn (6) and (7).

$$\text{OPTR} = \frac{\text{Slope}}{A} \tag{6}$$

$$\text{OP} = \text{OPTR} \times \frac{x}{\Delta P} \tag{7}$$

where A = area of the film, ΔP = difference between the partial vapor pressure of the Milli-Q water and dry atmosphere (0.02308 atm. at 25 °C), and x = film thickness (m).

2.3.10. Soil burial test. The soil burial test was carried out according to the previously reported method with some modifications[14] for 10 days. Film samples with dimensions of 20 × 20 mm taken for analysis were preheated in an oven at 70 °C for 24 h, and the initial dry mass was recorded as W_1. The dried film samples were then buried in soil and were watered once a day with water. After ten days, the films were isolated, gently washed with Milli-Q water and dried in an oven at 70 °C for 24 h. They were cooled in a desiccator and the final weight of the samples was recorded as W_2. The degradation percentage of the film samples was calculated using eqn (8).

$$\text{Degradation}(\%) = \frac{W_1 - W_2}{W_1} \times 100 \tag{8}$$

where W_1 = initial dry weight and W_2 = dry weight of the sample after degradation.

2.3.11. Assessment of the antimicrobial efficacy. The antimicrobial efficacy of the control and active films was assessed against *E. coli* (ATCC 10799), *S. aureus* (ATCC 6538), *B. subtilis* and *C. albicans* (ATCC 24433). The sample solutions were prepared by dissolving films in 1% acetic acid (1 mg mL^{-1}). Pure bacterial cultures were subcultured in Luria broth (LB) media until the absorbance at 600 nm reached 0.5. The broth culture was spread using a swab on the MHA dishes (4 mm in thickness), followed by the introduction of 100 μL of the prepared sample solutions into wells (8 mm in diameter) made with a gel puncher. Petri dishes were incubated at 37 °C overnight. The inhibition zone was recorded using a Vernier scale.[14,33]

2.3.12. Antioxidant activity. The antioxidant activity of the control and active films was evaluated using the DPPH (2,2-diphenyl-1-picrylhydrazyl) free radical scavenging assay.[34] In short, standard ascorbic acid solutions of 100–500 μL and sample solutions of 1 mg mL^{-1} were diluted to 1000 μL with methanol, followed by treatment with 500 μL methanolic DPPH (0.5 mM), and incubated in the dark at room temperature for 30 min. The absorbance at 517 nm was determined in a UV-visible spectrophotometer (Labman, LMSP UV-1200), using DPPH diluted with methanol as a control and methanol alone as the blank solution. The DPPH free radical scavenging activity was calculated using eqn (9), which was expressed in terms of the percent inhibition.

$$\text{DPPH free radical scavenging activity}(\%) = \frac{\text{Ab}_c - \text{Ab}_s}{\text{Ab}_c} \times 100 \tag{9}$$

where Ab_c = absorbance of control and Ab_s = absorption of the sample.

2.3.13. Overall migration studies. The overall migration test was performed according to ASTM standard IS:9845-1998 using three food stimulants: distilled water, 50% ethanol and 3% acetic acid. In brief, 20 × 20 mm films were immersed in beakers containing 30 mL of food simulants, and placed in a hot air oven for 10 days at 40 °C. The impact of the food stimulants on alcoholic, acidic and watery food items was evaluated gravimetrically, and the results were expressed in terms of mg dm^{-2}.[2] The amount of extractive was calculated according to eqn (10).

$$\text{Amount of extract} = \frac{M}{V} \times 1000 \tag{10}$$

where M = mass of residue in mg minus blank value and V = total volume in mL of simulant used in each replicate.

2.4. Packaging efficiency of active films

The efficiency of the prepared AMC active films for food packaging applications was assessed using green grapes. The packaging test was performed at room temperature for 17 days. The fresh green grapes purchased from the local market were cleaned with Milli-Q water and packed in pouches made from AMC active films. Unpacked grapes were treated as a control. The freshness and extension of the shelf life of green grapes were monitored.

2.4.1. Weight loss analysis. Weight loss of the grapes, unpacked and packed with AMC active films, was determined by weighing the grapes on the 1st, 5th, 10th, 15th, and 17th days during the storage period. Findings were presented in terms of the percentage of weight loss with respect to the initial weight.[35]

2.4.2. Antibrowning analysis. The extinction value method was used to determine the browning degree of grapes.[36] The test was performed after 17 days of storage. In brief, 20% (w/v) of the grape sample solution was prepared by mixing the grape with cold steamed water. The absorbance of the sample solution was recorded at 410 nm. The browning degree was expressed as A_{410nm} (absorbance at 410 nm).

2.5. Statistical analysis

All of the tests were performed in triplicate, and the data were presented as an average value with their standard deviation (average value ± SD). Statistical analysis was performed using Origin-9 software *via* one-way ANOVA. Tukey's test was performed to distinguish the average values at the $p \leq 0.05$ significance level.

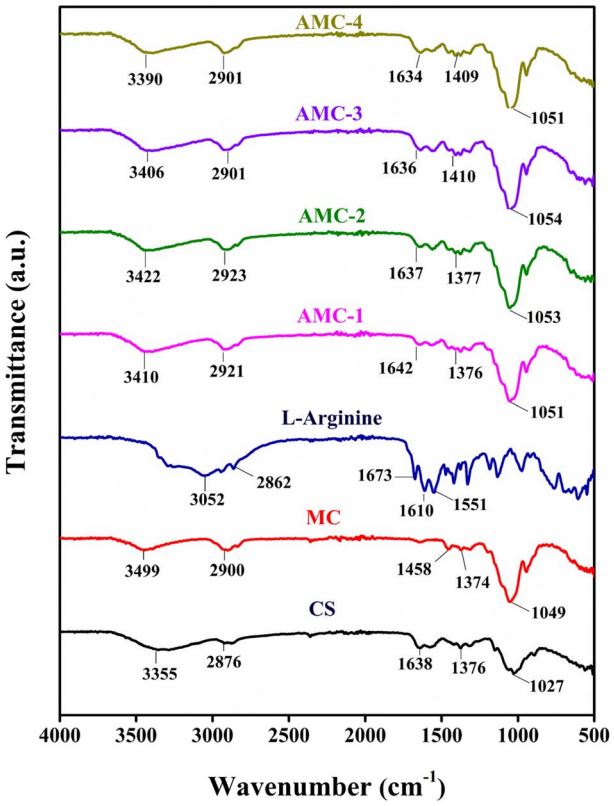

Fig. 1 FTIR spectra of CS, MC, L-arginine, AMC-1 (control) and AMC-2, AMC-3, AMC-4 active films.

3. Results and discussions

3.1. Fourier transform infrared spectroscopy (FTIR)

FTIR spectroscopy was used to investigate the interactions between the functional groups of the polymer matrix and the active ingredient. The resulting spectra are shown in Fig. 1. The FTIR spectra of chitosan and methylcellulose show characteristic peaks at 1027 cm^{-1} and 1049 cm^{-1}, respectively, assigned to the C–O stretching frequency. This band was shifted to 1051 cm^{-1} in the AMC-1 (control) film. Furthermore, the stretching frequency at 1638 cm^{-1} related to the –(NH_2) group of the CS was shifted to 1642 cm^{-1} owing to the interaction between the hydroxyl group of MC and the amine group of CS, confirming the compatibility of CS and MC in the active film.[37] The absorption peaks at 1673 cm^{-1} and 1610 cm^{-1} in the FTIR spectrum of L-arginine are attributed to the stretching vibration of the carboxyl carbonyl and guanidine groups of L-arginine, respectively.[38,39] The slight decrease in the peak intensities of the –NH and –OH groups can be observed in the spectra of the L-arginine-incorporated AMC active films, reflecting the reduction in the content of hydroxyl and amine groups.[39] The absorption bands at 3410 cm^{-1}, 2921 cm^{-1},1642 cm^{-1} and 1051 cm^{-1} were migrated to 3390 cm^{-1}, 2901 cm^{-1}, 1634 cm^{-1}, and 1054 cm^{-1}, respectively, due to the intermolecular interaction between the components of the polymer matrix through hydrogen bonding.[18,40] Furthermore, the characteristic absorption peak around 1634–1637 cm^{-1}, observed in L-arginine-incorporated AMC active films, is associated with the presence of the guanidine group, indicating that L-arginine is successfully linked to the polymer backbone.[41] In addition, the stretching peak at 1642 cm^{-1} associated with the AMC-1 (control) film corresponds to the –C═O stretching of the amide-I group, and decreased towards a lower wavenumber at 1637 cm^{-1} (AMC-2), 1636 cm^{-1} (AMC-3), and 1634 cm^{-1} (AMC-4) with the inclusion of L-arginine, indicating physical interactions between the components of the polymer matrix and L-arginine.[42] Band shifts in FTIR spectra indicate physical and chemical interactions within the polymer matrix, with slight variations indicating physical interactions and significant shifts suggesting chemical interactions. In this study, the FTIR spectra revealed slight variations in frequency, indicating a physical interaction between L-arginine and the components of the polymer matrix, rather than a chemical interaction.

3.2. Surface morphology

The morphological features of the active films rely on the interactions between the functional groups of the polymer matrix and active ingredients, which impact the active films' physical, optical, and barrier properties. The SEM micrographs of the AMC control and active films are presented in Fig. 2. The surface of AMC-1 (control) film appeared slightly rough and non-uniform but still exhibited compact and nonporous structure. These observations indicate the good compatibility between the components of the MC/CS matrix.[43] Incorporation of L-arginine substantially improved the surface morphology of the AMC active films. Furthermore, the increase in the L-arginine content presented a more regular and dense texture, reflecting that L-arginine has been well dispersed into the polymer matrix without any phase separation and agglomeration.[44] The AMC-4 active film showed a smooth and homogeneous surface, indicating compatibility among the polymer matrix components. Overall, the surface morphology of all of the AMC active films revealed compact and continuous textures that altered the physical and mechanical parameters of the film. Thus, including L-arginine improved the surface morphology of the AMC active films.[20]

3.3. X-ray diffraction (XRD)

X-ray diffraction analysis was performed to inspect the microcrystalline structure of the AMC active films. The X-ray diffractograms of L-arginine, and the AMC control and active films are presented in Fig. 3. The AMC control and active films exhibited two major crystalline peaks at around 8° and 20°. These peaks indicate the semicrystalline nature of the active films.[45] According to the results, the peak registered at around $2\theta = 20°$ was found to be the crystalline peak of CS, while the peaks located at around $2\theta = 8°$ and 20° corresponded to the crystalline peaks of MC.[37] The XRD diffractogram of L-arginine shows sharp and well-defined characteristic diffraction peaks at specific 2θ angles, indicating its crystalline nature, which is in agreement with previously reported literature.[46] Moreover, the peak intensity of the AMC-1 (control) film was increased with L-arginine incorporation, indicating that the degree of

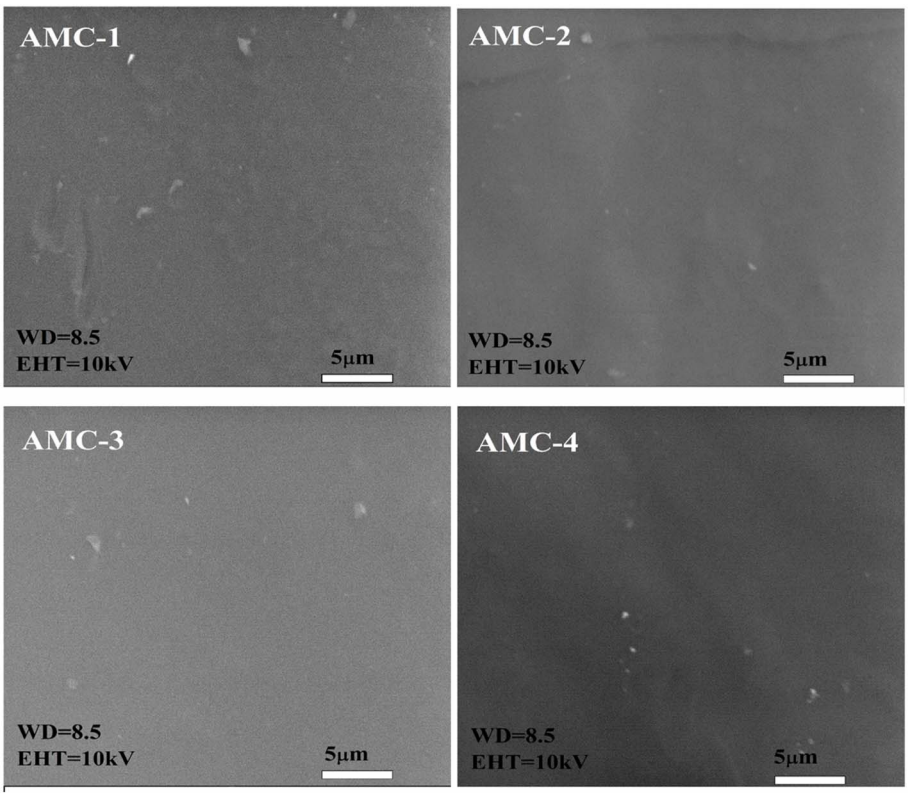

Fig. 2 SEM images of the AMC-1 (control) and AMC-2, AMC-3, and AMC-4 active films.

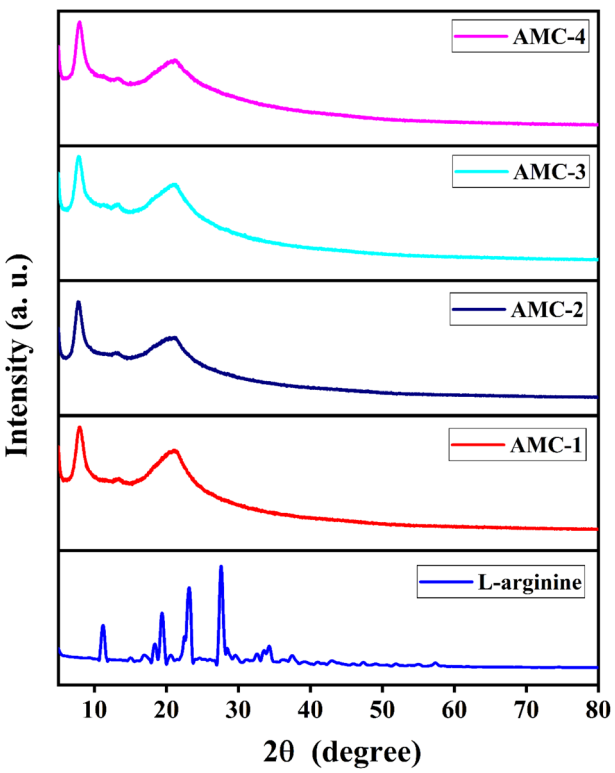

Fig. 3 X-ray diffraction patterns of the AMC-1 (control) and AMC-2, AMC-3, and AMC-4 active films.

crystallinity was improved by the addition of L-arginine [37,47]. The variation in the % crystallinity of the active films as a result of the incorporation of L-arginine is presented in Table 1. The findings illustrate that the AMC-1 (control) film without L-arginine has the lowest crystallinity compared to the AMC-2 and AMC-3 active films. Meanwhile, the crystallinity of the active films increased with an increase in the L-arginine content. This could be attributed to the presence of four amine groups in the L-arginine molecule, which facilitated the intermolecular hydrogen bonding interaction within the polymer matrix, thereby influencing the crystallinity.[41,47,48] Overall, the AMC active films exhibited increased crystallinity compared to the AMC-1 control film.

3.4. Mechanical properties

Fabricated active films must have sufficient mechanical properties for food packaging applications to retain their ability to endure stress during storage and transportation, which reduces the risk of damage and scratches.[29] Fig. 4(a and b) depicts the results of the mechanical properties of the fabricated active films. The results show that the AMC-1 (control) film exhibited a tensile strength of 37.81 ± 0.68 MPa and 11.32% ± 0.36% elongation at break. Both tensile strength and elongation at break were significantly improved by incorporating L-arginine, and reached a maximum value of 41.11 ± 1.03 MPa and 14.11% ± 0.53%, respectively, with an L-arginine content of 5.0%. This improved tensile strength was attributed to the intermolecular hydrogen bonding interaction between the functional groups of

Table 1 Thickness, crystallinity, water vapour transmission rate (WVTR), oxygen permeability (OP) and soil degradation rate of AMC-1 (control) and AMC-2, AMC-3, AMC-4 active films[a]

Samples	Thickness (mm)	Crystallinity (%)	WVTR (g m^{-2} h^{-1})	OP × 10^{-5} ($cc^3 \cdot m^{-1} \cdot 24\ h \cdot atm$)	Degradation rate (%)
AMC-1	0.080 ± 0.001^{a}	47.05 ± 0.50^{d}	27.49 ± 1.01^{a}	11.6 ± 0.20^{a}	20.94 ± 0.62^{b}
AMC-2	0.078 ± 0.003^{a}	49.28 ± 0.33^{c}	26.64 ± 0.57^{a}	10.4 ± 0.12^{b}	27.53 ± 0.72^{a}
AMC-3	0.077 ± 0.001^{a}	51.56 ± 0.22^{b}	26.21 ± 0.92^{a}	10.1 ± 0.07^{bc}	28.23 ± 0.43^{a}
AMC-4	0.081 ± 0.004^{a}	54.09 ± 0.16^{a}	25.45 ± 1.55^{a}	9.6 ± 0.19^{c}	28.88 ± 0.89^{a}

[a] Data are presented as mean ± SD [a–d]. The superscript letters in every datapoint indicate statistically significant differences ($P < 0.05$).

the MC/CS matrix and the $-NH_2$ of L-arginine and the cooperative hydrogen bonding effect of L-arginine. The incorporated L-arginine facilitated interchain linkage by forming hydrogen bonds with the functional groups of components of the polymer matrix, which hindered the mobility of the polymer network.[39,49] These findings are also consistent with FTIR studies, which indicated that the wavenumber associated with –OH groups has decreased.

In contrast, the percentage elongation at break was also slightly enhanced. The increased elongation at break, ascribed to the plasticizing effect of glycerol, led to increased free volume in the polymer matrix.[50] These findings were supported by the results reported by Narasagoudr *et al.* (2020),[26] that elongation at break values of the rutin-induced CS/PVA film were enhanced with rutin content. However, at a higher weight percentage of L-arginine (AMC-4), the tensile strength and elongation at break values decreased, which might be due to the significant impact of the film thickness on the mechanical properties, as the thickness has an inverse relationship with the tensile properties. Hence, the mechanical properties decreased with increased film thickness. Abdel-Mohti *et al.* (2015)[51] reported that the mechanical characteristics of the films increased with a decrease in the film thickness, showing that the mechanical properties are strongly reliant on the thickness of the films. The findings are consistent with the results reported by Hiremani *et al.* (2021),[29] indicating that both tensile strength and elongation at the break values of the chitosan film were decreased at a higher content of *Curcuma zedoaria* powder.

3.5. Surface wettability

Water contact angle (WCA) measurements were carried out to inspect the surface wettability of the fabricated control and active films. The images and degree of contact angle values are displayed in Fig. 5. Generally, films with a WCA < 65° are considered hydrophilic, whereas films with a WCA > 65° are considered hydrophobic.[43] The AMC-1 (control) film exhibited surface hydrophobicity with a WCA of 90.6° ± 0.21 owing to the hydrophobic domain of the CS. It was found that the WCA of the AMC active films was decreased by incorporating L-arginine compared to the AMC-1 (control) active film. Furthermore, a decrease in the WCA degree of the active films was observed as the weight percent of L-arginine increased. This resulted in a decreased surface hydrophobicity of the active films, which might be attributed to the free polar moieties available on the film surface, facilitating the interaction with the water molecules.[21] The AMC-4 active film with the highest L-arginine content exhibited a lower water contact angle. This decrease in

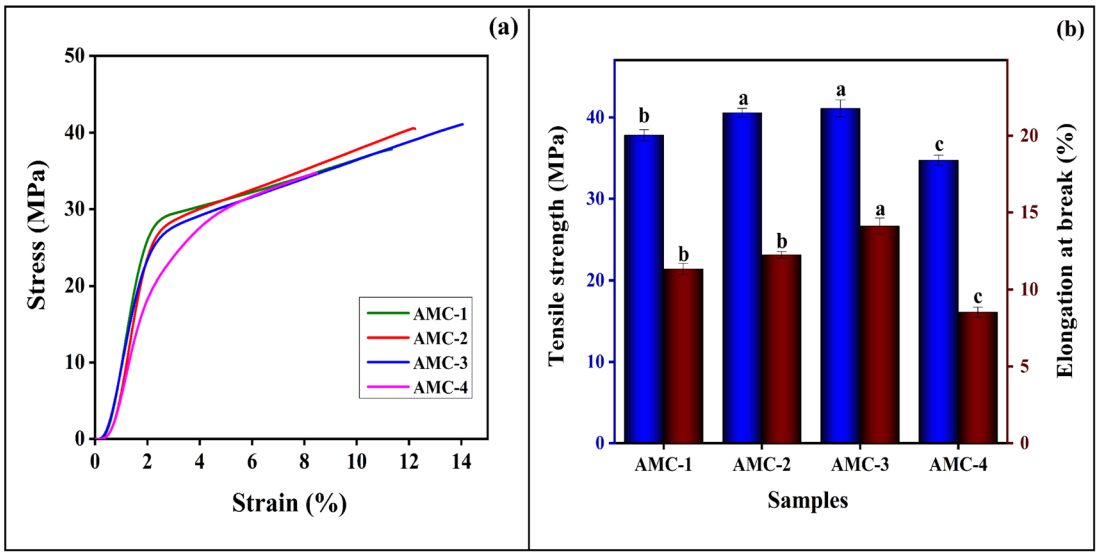

Fig. 4 Mechanical properties: (a) stress–strain curve, (b) tensile strength and elongation at break of the AMC-1 (control) and AMC-2, AMC-3, AMC-4 active films.

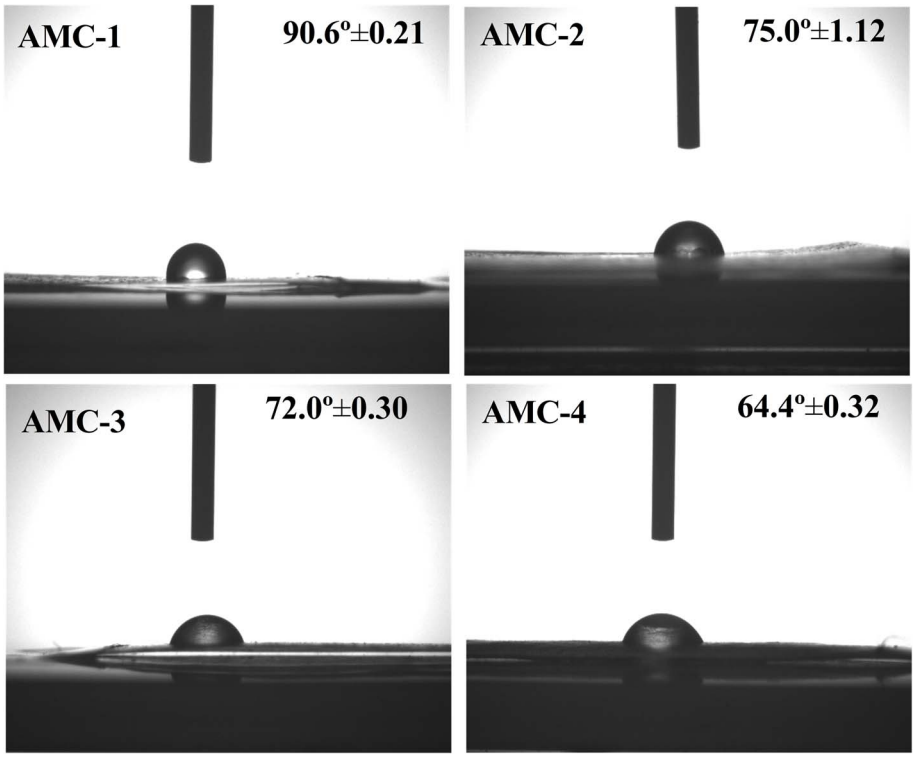

Fig. 5 Water contact angle images of the AMC-1 (control) and AMC-2, AMC-3, and AMC-4 active films.

water contact angle is due to the hydrophilic nature of L-arginine.[52]

3.6. Moisture adsorption and water solubility

The majority of biopolymers are sensitive to moisture. Hence, the moisture absorption study is accepted as a fundamental characteristic for food packaging applications.[53] The moisture adsorption capacity of the films was evaluated, and the results are depicted in Fig. 6(a). The obtained results demonstrated that the moisture adsorption capacity of the AMC-1 (control) film was 2.53% ± 0.05, which was increased by the addition of L-arginine.[54] Furthermore, the moisture adsorption capacity of the AMC active films increased from 2.95% ± 0.11 to 3.03% ± 0.07 as the concentration of L-arginine was raised. The improved MA values were attributed to the greater solubility and hydrophilic character of L-arginine, which resulted in free polar sites that facilitated the clustering of water molecules on the film surface.[55] Among all the films, AMC-4 with a high content of arginine (7.5 wt%) exhibited the highest moisture

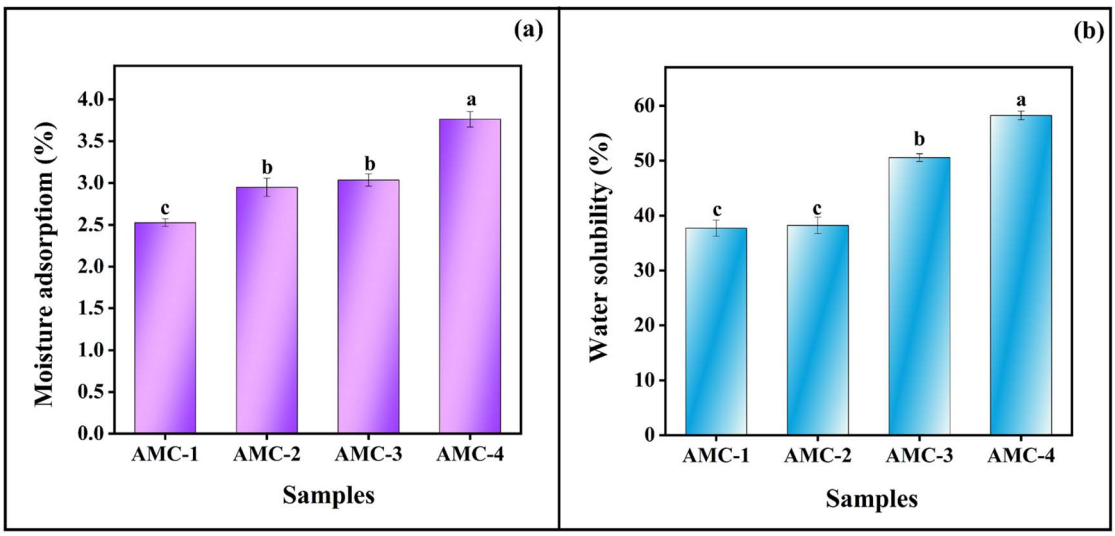

Fig. 6 (a) Moisture adsorption, and (b) water solubility values of the AMC-1 (control) and AMC-2, AMC-3, and AMC-4 active films.

adsorption value (3.76% ± 0.09), which may be related to the fact that water molecules occupied the free sites that were available on the film's surface.[56]

Water solubility significantly impacts the biodegradability of films when the films are employed as a packaging material. Higher film solubility influences the degradation of films, whereas partial or low solubility is best suited for storage. The outcomes of the percentage of water solubility of the fabricated active films are presented in Fig. 6(b). The AMC-1 (control) film showed a low WS of 37.75% ± 1.47, compared to other active films, owing to the insolubility of chitosan in the blend films at neutral pH. The incorporation of L-arginine into the MC/CS matrix improved the solubility of the AMC active films in water. This is due to the hydrophilic nature and positively charged guanidium side chain of L-arginine, which possesses a high pK_a of 12.48 in a neutral pH environment.[54,57] Additionally, the film solubility was enhanced from 38.26% ± 1.51 to 50.57% ± 0.70 as the concentration of arginine was raised from 2.5 to 5.0 (wt%). The AMC-4 active film with 7.5 wt% of arginine exhibited the highest water solubility of 58.27% ± 0.79. This could be explained by the interaction between the carboxylic acid groups of L-arginine and an amine on the glucosamine unit of chitosan with an increased degree of substitution, which led to a reduction in the $-NH_2$ groups and an increase in the number of hydroxyl groups.[58] These accessible free hydroxyl groups interact with water molecules through hydrogen bonding, enhancing the film's water solubility.[14]

3.7. UV-visible spectroscopy analysis

One of the most desirable parameters of packaging film is that it should safeguard the food from ultraviolet radiation. UV radiation promotes numerous detrimental activities that diminish the nutritional quality of food products.[59,60] As illustrated in Fig. 7(a), the percentage transmittance of the AMC-1 (control) film dropped with the incorporation of L-arginine, and continued to decline as the weight percentage of L-arginine increased. Furthermore, AMC active films containing different weight percentages of L-arginine exhibited higher absorption and UV light barrier qualities than the AMC-1 (control) film. L-arginine incorporation restricted the transmission of ultraviolet light below 370 nm, and lowered the % light transmittance across all the spectral regions.[61] This may be attributed to secondary interactions between the polymer matrix and L-arginine that resulted in a compact molecular structure, as evidenced by SEM and FTIR studies, which altered the light transmission rate through active films.

The UV barrier characteristics of the active films were evaluated between the wavelength range of 315–400 nm (UV-A), 280–315 nm (UV-B), and 200–280 nm (UV-C), and the graph is presented in Fig. 7(b). Lipid oxidation occurs most frequently in the 200–315 nm wavelength range.[59] With the addition of (7.5 wt%) L-arginine, the % transmittance of the AMC-1 (control) film dropped from 10.03% to 1.67% at 315 nm, and from 50.21% to 21.98% at 400 nm. Thus, adding L-arginine to the polymer matrix enhanced the barrier property through the absorption of UV light.[60,61] The UV barrier property of the AMC active films is superior to that observed in a study published by Gasti *et al.* (2020),[62] demonstrating that *Solanum nigrum* leaf extract-added CS/PVA films exhibited good ultraviolet (310 nm) barrier properties. The opacity values of the AMC active films at 250 nm, 300 nm and 350 nm with respect to the UV-A, UV-B, and UV-C regions, respectively, are shown in Fig. 7(b). The opacity of the L-arginine-incorporated AMC active films was higher than that of the AMC-1 (control) film, which could be attributed to a reduction in the % light transmittance. However, the improved opacity values of the active films help to prevent lipid oxidation and preserve the nutritional qualities of packaged food.[63] In the present study, the opacity value of the active films increased as the weight percentage of L-arginine was increased. The AMC-4 active film with a high L-arginine content exhibited a maximum opacity value of 27.64 ± 0.13 at 250 nm in the UV-C region, in contrast to the AMC-1 (control) film. The increments

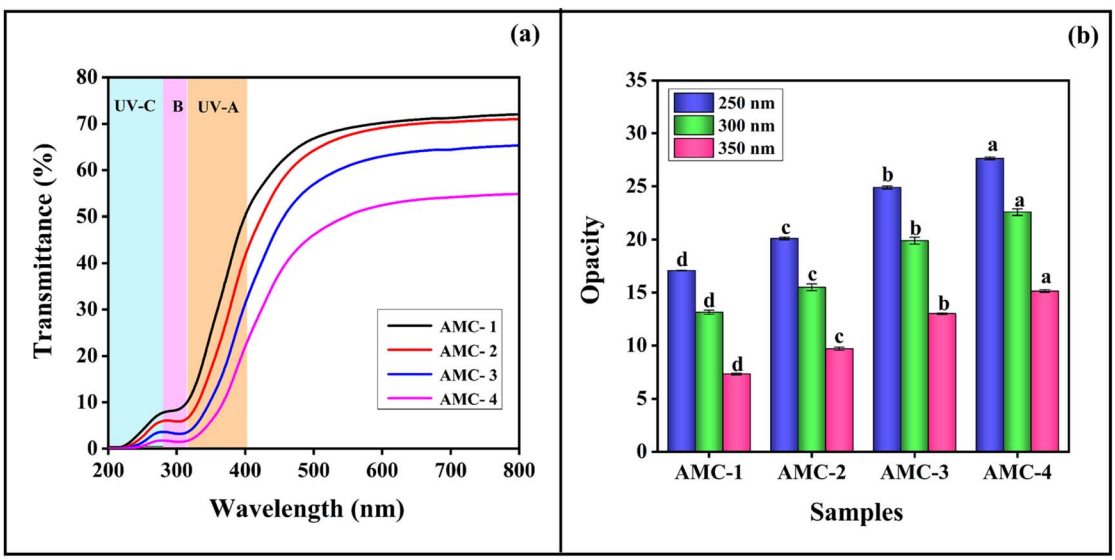

Fig. 7 Optical parameters: (a) % transmittance, (b) opacity of the AMC-1 (control) and AMC-2, AMC-3, AMC-4 active films.

in the opacity values might be due to the compact structure of the active films induced by the secondary intermolecular interaction between the polymer matrix and L-arginine that decreased the interchain gap, thereby permitting less light to transmit through the active films.[64]

3.8. Water vapour transmission rate (WVTR)

Examining water barrier properties is essential for packaging applications, as it provides information on the diffusivity rate of water vapors from the external atmosphere to packed food products *via* the packaging.[65] Proper water vapor barrier properties of the packaging film can preserve the quality and prolong the life span of the food products. The presence of moisture content in the food may promote a variety of enzymatic and chemical reactions, diminishing the functional qualities of food and reducing the food products' lifespan.[66] The WVTR results of the fabricated control and active films are shown in Table 1. Initially, the AMC-1 (control) film showed a WVTR of 27.49 ± 1.01 g m^{-2} h^{-1}. However, including L-arginine in the MC/CS polymer matrix significantly lowered the diffusivity rate of water vapors to 26.64 ± 0.57 g m^{-2} h^{-1} through the AMC-2 active film. When the weight percentage of L-arginine continued to increase, the rate of water vapour transmission through the AMC-3 and AMC-4 active films declined to 26.21 ± 0.92 g m^{-2} h^{-1} and 25.45 ± 1.55 g m^{-2} h^{-1}, respectively, compared to the AMC-1 (control) film. The decrease in the WVTR was due to the complex and dense surface morphology, as witnessed by the SEM micrographs. This compact molecular structure introduced the tangled path, which lengthened the permeation path of water vapors and reduced the diffusivity rate of vapors through active films,[49,67] as shown in Fig. 8.

3.9. Oxygen permeability (OP)

The oxygen barrier performance of packaging materials is essential for food packaging applications since oxygen transmission within the material promotes food oxidation, leading to food spoilage. Table 1 presents the oxygen permeability values of the control and active films. An oxygen permeability of 11.6 × 10^{-5} ± 0.20 cc·m^{-1}·24 h·atm was noted for the AMC-1 (control) film, which was decreased by incorporating L-arginine. Furthermore, it was observed that with increased L-arginine content, the OP of the AMC active film was significantly reduced. Meanwhile, the AMC-4 active film showed strong oxygen barrier performance with a lower OP of 9.6 × 10^{-5} ± 0.19 cc·m^{-1}·24 h atm compared to the AMC-1 (control) film. The enhanced oxygen barrier performance of the active films was due to the more compact, tightened structure resulting from the compatibility of the L-arginine with the film matrix, which made it more difficult for nonpolar oxygen molecules to pass across the film, as shown in Fig. 8.

3.10. Soil burial test

The degradation of active films in soil takes place in two steps. In the initial step, swelling of polymer films is caused by the penetration of water into the films, which influences the growth of microorganisms. The second step includes disruption of polymer films, followed by weight loss as a result of enzymatic and secreted degradation.[68] In the present work, the degradation rate of the fabricated active films in soil was examined, and the resulting data are illustrated in Table 1. All of the active films showed more than 20% soil degradation within 10 days. The AMC-1 (control) film showed 20.94% ± 0.62 degradation, while the degradation rate of the L-arginine-incorporated AMC active films is greater. The AMC-4 active film exhibited 28.88% ± 0.89 soil degradation within 10 days. In comparison to the AMC-1 (control) film, this faster soil degradation might be due to the decay of small units of active films by the action of microorganisms owing to the high water solubility of films, as evidenced by the water solubility results. These results were supported by Carissimi, Flores and Rech (2018),[69] who reported that films exhibiting high water solubility were likely to undergo fast biodegradation.

3.11. Antimicrobial efficacy

The antimicrobial efficacy of the control and active films was assessed against Gram-negative bacteria *E. coli*, and Gram-positive bacteria *S. aureus*, *B. subtilis*, and fungi *C. albicans*.[70] The antimicrobial activity and respective inhibition zones are displayed in Fig. 9 and Table 2. All of the prepared active films

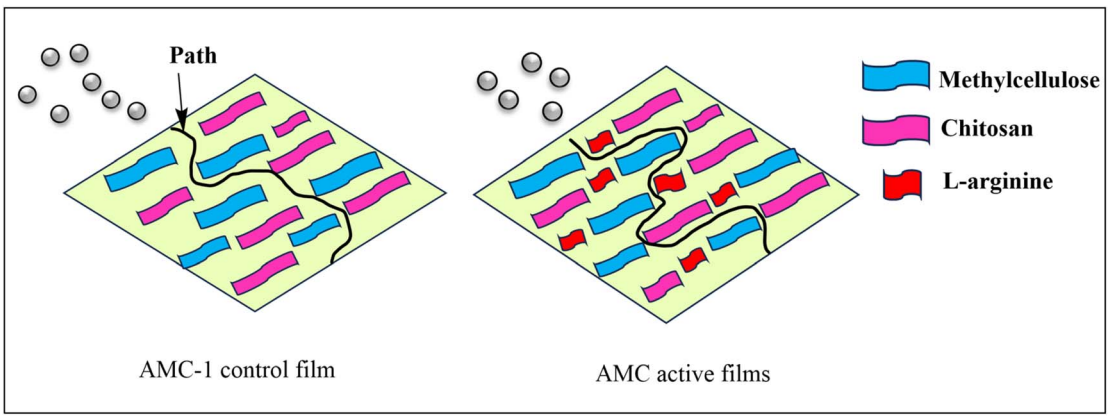

Fig. 8 Representation of the plausible scheme for the decreased WVTR and OP.

exhibited potent antimicrobial efficacy against *S. aureus* and *B. subtilis*, and showed less activity against *E. coli*. The antimicrobial efficacy of the control and active films is due to the microbial inhibiting ability of CS. However, the precise mechanism of the intrinsic antimicrobial efficacy of the CS is unknown.[26] It was noticed that the AMC active films suppressed the activity of *B. subtilis* and *S. aureus* more efficiently than *E. coli*. This significant difference in microbial inactivation is attributed to the variance in the cell wall compositions of the Gram-positive and Gram-negative bacteria. The outer layer of Gram-negative bacteria comprises phospholipids and lipopolysaccharides, which can hinder antibacterial activity, making Gram-negative bacteria resistant to the antimicrobial compound. The Gram-positive bacteria lack this essential outer lipid layer, and are less resistant to antimicrobial ingredients.[71] Also, considerable antifungal activity was observed against *C. albicans.* Incorporating L-arginine in the MC/CS polymer matrix further improved the antimicrobial properties of the AMC active films. This improved antimicrobial activity is due to the positively charged amino and guanidyl groups in L-arginine that attack the anionic constituents of the bacterial cell wall *via* electrostatic interaction. Disturbing the physiological activity of microbes and disrupting the microbial membrane through a lytic mechanism that releases cell constituents eventually causes cell death.[38,72]

Table 2 Antimicrobial zone (zone of inhibition in mm) of the AMC-1 (control) and AMC-2, AMC-3, AMC-4 active films[a]

	Zone of inhibition (mm)			
Samples	*B. subtilis*	*S. aureus*	*E. coli*	*C. albicans*
AMC-1	16.0 ± 0.17^{d}	16.0 ± 0.28^{b}	8.5 ± 0.17^{c}	11.5 ± 0.11^{c}
AMC-2	17.5 ± 0.28^{c}	17.5 ± 0.40^{a}	9.5 ± 0.23^{b}	13.0 ± 0.23^{b}
AMC-3	19.5 ± 0.11^{b}	18.0 ± 0.34^{a}	10.0 ± 0.28^{b}	13.5 ± 0.17^{b}
AMC-4	21.0 ± 0.23^{a}	18.5 ± 0.23^{a}	11.0 ± 0.11^{a}	14.5 ± 0.28^{a}

[a] Data are presented as Mean ± SD, [a–d]. The superscript letters in every data point indicate that there is a significant difference ($P < 0.05$).

3.12. Antioxidant activity

Food packaging materials must mitigate the oxidation of food ingredients, such as proteins, lipids and fatty acids, which promote food spoilage. Hence, antioxidant packaging materials prolong the shelf life of packaged foods. It was found that the antioxidant efficacy is predominantly attained by suppressing the production of free radicals. Thus, radical scavenging activity may play a significant role in the antioxidant process.[73,74] The results of the antioxidant response of AMC active films are depicted in Fig. 10. The AMC-1 (control) film showed negligible antioxidant activity, whereas incorporating L-arginine into the

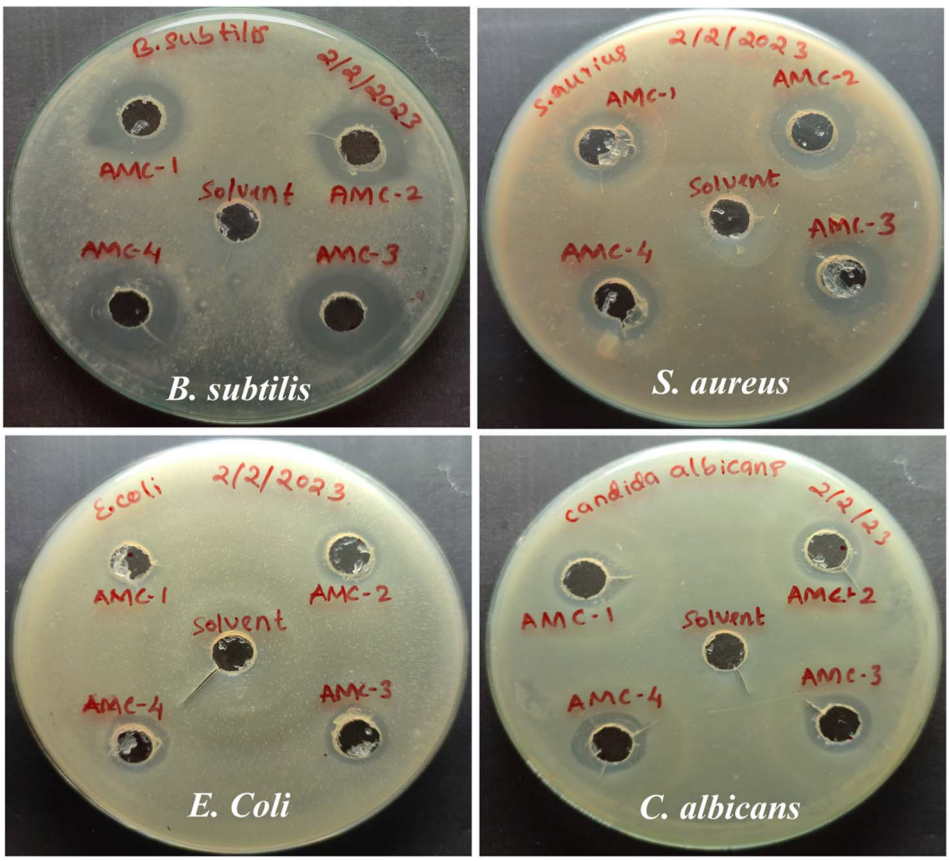

Fig. 9 Demonstration of the antimicrobial activity of the AMC-1 (control) and AMC-2, AMC-3, and AMC-4 active films against *B. subtilis*, *S. aureus*, *E. coli* and *C. albicans*.

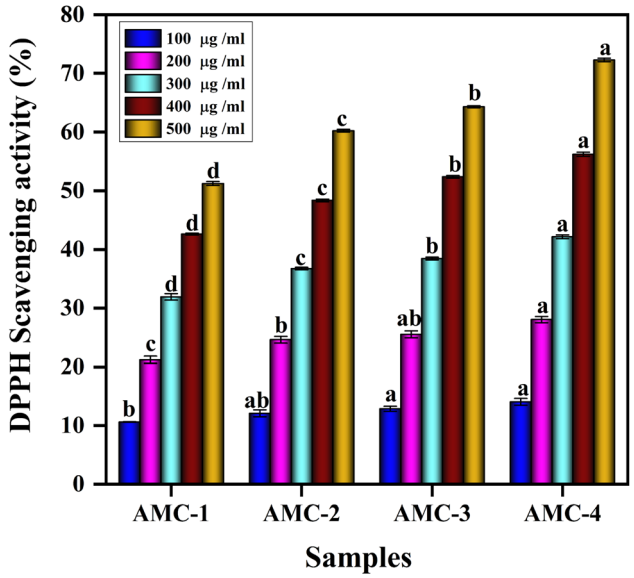

Fig. 10 Antioxidant activity profile of the AMC-1 (control) and AMC-2, AMC-3, and AMC-4 active films.

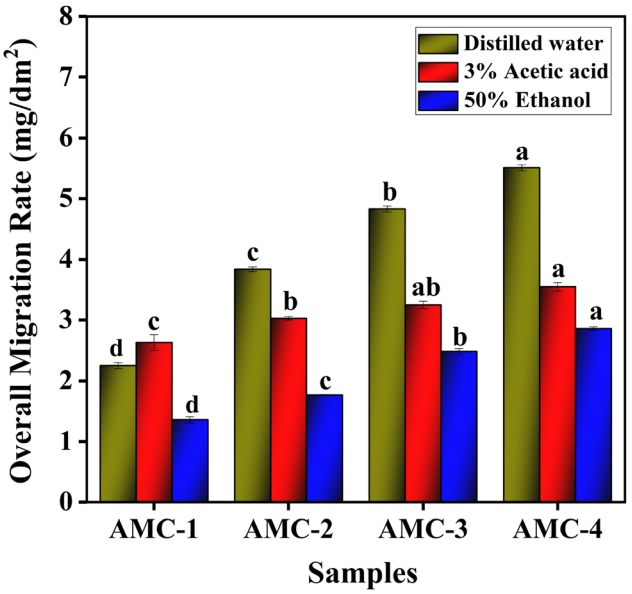

Fig. 11 Results of the overall migration of the AMC-1 (control), and AMC-2, AMC-3, AMC-4 active films.

MC/CS polymer matrix improved their antioxidant potential. The free radical scavenging activity was promoted as the weight percentage of L-arginine was increased. This improved radical scavenging activity may be attributed to the interaction of the incorporated L-arginine with free radicals *via* the donation of electrons and the development of the free radical chain process. The AMC-4 active film with a higher L-arginine weight percentage (7.5%) displayed greater antioxidant potential, possibly related to the higher electron density of functional moieties on the active films. Increased electron cloud density accelerates the donation of electrons, promoting the free radical scavenging process.[73] Therefore, it was evident that the incorporation of L-arginine enhanced the accessibility of potential electron-donating groups in the AMC active films, resulting in more significant antioxidant activity in comparison to the AMC-1 (control) film.

3.13. Overall migration rate

An overall migration test was carried out using three food stimulants, such as water, 50% ethanol and 3% acetic acid, to evaluate the compatibility of the active films with aqueous, alcoholic beverages and acetic food products, respectively. The migration of packed material into the food stimulants leads to contamination of the food packed in it, and causes health problems due to consuming these packed food products. The Bureau of Indian Standards (IS:9845-1998) declared that the overall migration of the packing material should be less than 10 mg dm^{-2}. Fig. 11 displays the results of the overall migration rate. The findings revealed that the overall migration values of active films in all three food stimulants were within the permissible limit of 10 mg dm^{-2}, suggesting their food compatibility. The overall migration values rely on thermodynamic properties like the swelling polarity, film solubility and the interaction between the components of the polymer matrix and the food stimulants. In the present study, the active films exhibited the highest overall migration rate in distilled water compared to 3% acetic acid and 50% ethanol, owing to the high solubility of L-arginine in water. Among other food stimulants, the migration rate is higher in 3% acetic acid due to chitosan's solubility in acetic acid. It has been found that the overall migration of active films increased as the content of L-arginine in the polymer matrix increased. This could be attributed to the swelling behavior of the active films in all three food stimulants, which tends to increase the free volume of the MC/CS polymer matrix and influences the release of L-arginine from the polymer matrix.[18]

3.14. Packaging efficiency of the active films

3.14.1. Visual appearance. The visual appearance of the green grapes unpacked and packed with AMC active films over the storage period of 17 days is shown in Fig. 12(a). Initially, all the grape samples packed with AMC active films, including the unpacked ones, had a good appearance and were green. When the storage period was extended up to the 5th day, the unpacked grapes shriveled, began to turn brown and worsened on the 15th day of storage. The shrinkage and browning might be due to the dehydration and oxidation of polyphenols present in the grapes, respectively. The grapes packed in the AMC-1 film began to turn brown at the tip after the storage period of 10 days. In contrast, the grapes packed in the AMC-4 active film retained their physical appearance and colour even after the 15th day of storage. This is due to the enhanced antioxidant ability of the AMC-4 active film, which successfully mitigated the oxidizing activity of free radicals emitted on the surface of the grape and maintained the quality of the grape. Incorporating L-arginine into the MC/CS matrix improved the barrier characteristics, and the antimicrobial and antioxidant efficacy of the active films,

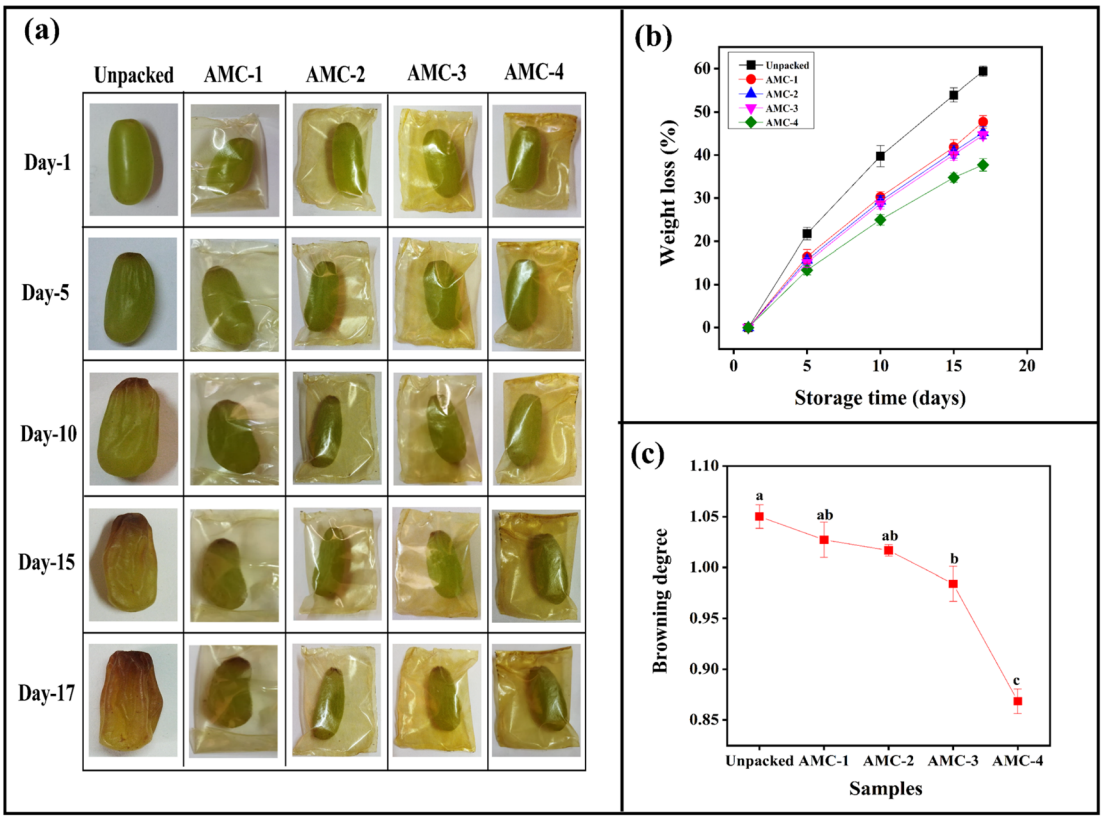

Fig. 12 (a) Monitoring freshness and shelf life, (b) percentage weight loss, and (c) antibrowning activity of unpacked and packed grapes in the AMC-1 (control), AMC-2, AMC-3 and AMC-4 active films.

which resulted in preserving the grape quality for a longer time period.[75] Hence, the L-arginine weight percentages in the films directly correlate to the efficacy of packaging grapes. Similar findings were published by S. Kumar *et al.* (2019); as the concentration of nanoparticles in the agar-ZnO NP matrix increased, the shelf life of green grapes was extended.[76]

3.14.2. Weight loss. The weight loss of unpacked green grapes and those packed in AMC active films are illustrated in Fig. 12(b). Generally, the weight loss of the fruits occurs due to the dehydration process caused by water loss through evaporation and cellular respiration throughout storage.[77] The weight loss results suggested that the weight loss of green grapes unpacked and packaged with AMC active films increased as the storage period increased. It was observed that the unpacked grape exhibited the highest weight loss, while the grape packed with the AMC-4 active film exhibited the most negligible weight loss during storage compared to those packed with other AMC active films. The reduction in weight loss of grapes packed with the AMC-4 active film was attributed to the improved barrier properties due to the presence of a higher weight percentage of L-arginine, as evidenced by the results of the WVTR, OP, UV barrier and antioxidant property, which delayed the water loss by modifying the internal atmosphere and prevented the weight loss.[35,77]

3.14.3. Antibrowning analysis. Colour is a crucial sensory parameter affecting the quality and visual appearance of grapes. However, browning occurs naturally due to enzymatic oxidation and microbial development throughout storage, which degrades the nutritional quality, shortens the shelf life and lowers the market value. Thus, browning is linked with antimicrobial and antioxidant activity.[78] Fig. 12(c) illustrates the browning degree of an unpacked grape and grapes packed with AMC active films. The findings showed that the browning degree of the unpacked grape was significantly higher than that of the grapes packed with AMC active films, which might be due to the oxidation of polyphenols and lipids present in the grapes. Meanwhile, the grape packed in the AMC-4 active film exhibited only the slightest browning. This suppressive action of the AMC-4 active film on the browning of the grape is attributed to several reasons. Firstly, it has an antibacterial property that mitigates the bacterial growth on the surface of the grapes. Secondly, the antioxidant efficacy of the AMC-4 active film safeguards the polyphenolic components in grapes against oxidation.[35] In addition, the film's UV barrier property prevents lipid oxidation, which in turn lowers the browning rate.

4. Conclusions

In the present work, active films of MC/CS were fabricated by incorporating L-arginine as an active ingredient using a sustainable solvent casting technique for green food packaging applications. FTIR analysis evidenced the hydrogen bonding interaction between L-arginine and the MC/CS film matrix. SEM results unveiled the dense and compact surface morphology with the addition of L-arginine. Incorporating L-

arginine affected the WS and MA properties, and significantly improved the mechanical (41.11 ± 1.03 MPa), UV barrier, water vapor barrier and oxygen barrier ($9.6 \times 10^{-5} \pm 0.19$) properties. Inclusion of L-arginine also enhanced the functional properties and biodegradability of the active films. Fabricated AMC active films exhibited potent antimicrobial and free radical scavenging activity. The AMC-4 active film showed higher antioxidant activity (72.28% ± 0.28) and antimicrobial efficiency than the AMC-1 (control) film. In addition, the grape packaging assessment indicated that the AMC-4 active film with a higher weight percentage of L-arginine (7.5%) maintained the grape quality throughout storage by controlling the weight loss and preventing the browning of the grape, and extended the shelf life of the grapes for up to 17 days. Hence, these findings reveal that fabricated L-arginine-functionalized AMC active films show strong potential as green packaging materials for food packaging applications.

Data availability

The data that supporting the findings of this study are available from the corresponding author upon reasonable request.

Author contributions

Suhasini Madihalli: conceptualization; data curation; formal analysis; methodology; visualization; resources; software; Roles: writing – original draft; review & editing. Saraswati P. Masti: the corresponding author; investigation; supervision; validation; writing – review & editing, visualization. Manjunath P. Eelager: investigation; formal analysis. Manjushree Nagaraj Gunaki: resources; investigation. Ravindra B. Chougale: validation, review & editing. Nagarjuna Prakash Dalbanjan: data curation, formal analysis. Praveen Kumar S. K.: formal analysis; review.

Conflicts of interest

The authors declare that there are no conflicts of interest.

Acknowledgements

The authors sincerely acknowledge the DST-SERB for aid in the purchase of UTM (Dr Saraswati P. Masti, Principal investigator under project sanctioned letter SB/EMEQ-213/2014, Dated: 29/01/2016) for the mechanical characteristics measurements and other laboratory facilities. The authors express their gratitude to the University Scientific Instrumentation Centre (USIC), DST – Sophisticated Analytical Instrument Facilities (DST-SAIF), for providing the necessary instrumental facilities. The authors also express their gratitude to the Principal and HOD of Chemistry, Karnatak Science College, Dharwad, for providing infrastructure facilities. One of the authors, Ms. Suhasini Madihalli, would like to thank the Government of Karnataka, India, for providing the Vidyasiri Research Studentship.

References

1 S. Mangaraj, A. Yadav, L. M. Bal, S. Dash and N. K. Mahanti, Application of biodegradable polymers in food packaging industry: A comprehensive review, *J. Packag. Technol. Res.*, 2019, **3**, 77–96, DOI: 10.1007/s41783-018-0049-y.

2 S. Bandyopadhyay, N. Saha, U. V. Brodnjak and P. Sáha, Bacterial cellulose and guar gum based modified PVP-CMC hydrogel films: Characterized for packaging fresh berries, *Food Packag. Shelf Life*, 2019, **22**, 100402, DOI: 10.1016/j.fpsl.2019.100402.

3 F. Wu, M. Misra and A. K. Mohanty, Challenges and new opportunities on barrier performance of biodegradable polymers for sustainable packaging, *Prog. Polym. Sci.*, 2021, **117**, 101395, DOI: 10.1016/j.progpolymsci.2021.101395.

4 J. Ahmed, M. Mulla, H. Jacob, G. Luciano, T. Bini and A. Almusallam, Polylactide/poly (ε-caprolactone)/zinc oxide/clove essential oil composite antimicrobial films for scrambled egg packaging, *Food Packag. Shelf Life*, 2019, **21**, 100355, DOI: 10.1016/j.fpsl.2019.100355.

5 S. Yildirim, B. Röcker, M. K. Pettersen, J. Nilsen-Nygaard, Z. Ayhan, R. Rutkaite, T. Radusin, P. Suminska, B. Marcos and V. Coma, Active packaging applications for food, *Compr. Rev. Food Sci. Food Saf.*, 2018, **17**, 165–199, DOI: 10.1111/1541-4337.12322.

6 Y. Liu, S. Ahmed, D. E. Sameen, Y. Wang, R. Lu, J. Dai, S. Li and W. Qin, A review of cellulose and its derivatives in biopolymer-based for food packaging application, *Trends Food Sci. Technol.*, 2021, **112**, 532–546, DOI: 10.1016/j.tifs.2021.04.016.

7 L. Kumar, D. Ramakanth, K. Akhila and K. K. Gaikwad, Edible films and coatings for food packaging applications: A review, *Environ. Chem. Lett.*, 2022, 1–26, DOI: 10.1007/s10311-021-01339-z.

8 L. Wu, C. Zhang, Y. Long, Q. Chen, W. Zhang and G. Liu, Food additives: From functions to analytical methods, *Crit. Rev. Food Sci. Nutr.*, 2022, **62**, 8497–8517, DOI: 10.1080/10408398.2021.1929823.

9 J. Bai, Y. Wu, K. Zhong, K. Xiao, L. Liu, Y. Huang, Z. Wang and H. Gao, A comparative study on the effects of quinic acid and shikimic acid on cellular functions of Staphylococcus aureus, *J. Food Protect.*, 2018, **81**, 1187–1192, DOI: 10.4315/0362-028X.JFP-18-014.

10 N. P. Dalbanjan, M. P. Eelager, K. Korgaonkar, B. N. Gonal, A. J. Kadapure, S. B. Arakera and S. P. Kumar, Descriptive review on conversion of waste residues into valuable bionanocomposites for a circular bioeconomy, *Nano-Struct. Nano-Objects*, 2024, **39**, 101265, DOI: 10.1016/j.nanoso.2024.101265.

11 N. P. Dalbanjan, M. P. Eelager and S. S. Narasagoudr, Microbial protein sources: A comprehensive review on the potential usage of fungi and cyanobacteria in sustainable food systems, *Food and Humanity*, 2024, **3**, 100366, DOI: 10.1016/j.foohum.2024.100366.

12 N. P. Dalbanjan and S. Praveen Kumar, A chronicle review of in-silico approaches for discovering novel antimicrobial

agents to combat antimicrobial resistance, *Indian J. Microbiol.*, 2024, **64**, 879–893, DOI: 10.1007/s12088-024-01355-x.

13 A. Kamari and E. Phillip, Chitosan, gelatin and methylcellulose films incorporated with tannic acid for food packaging, *Int. J. Biol. Macromol.*, 2018, **120**, 1119–1126.

14 M. P. Eelager, S. P. Masti, R. B. Chougale, V. D. Hiremani, S. S. Narasgoudar, N. P. Dalbanjan and P. K. SK, Evaluation of mechanical, antimicrobial, and antioxidant properties of vanillic acid induced chitosan/poly (vinyl alcohol) active films to prolong the shelf life of green chilli, *Int. J. Biol. Macromol.*, 2023, **232**, 123499, DOI: 10.1016/j.ijbiomac.2023.123499.

15 R. Priyadarshi, S.-M. Kim and J.-W. Rhim, Pectin/pullulan blend films for food packaging: Effect of blending ratio, *Food Chem.*, 2021, **347**, 129022, DOI: 10.1016/j.foodchem.2021.129022.

16 M. P. Eelager, S. P. Masti, R. B. Chougale, N. P. Dalbanjan and S. P. Kumar, Noni (Morinda citrifolia) leaf extract incorporated methylcellulose active films: A sustainable strategy for browning inhibition in apple slice packaging, *Int. J. Biol. Macromol.*, 2024, **269**, 132270, DOI: 10.1016/j.ijbiomac.2024.132270.

17 S. Yadav, G. Mehrotra, P. Bhartiya, A. Singh and P. Dutta, Preparation, physicochemical and biological evaluation of quercetin based chitosan-gelatin film for food packaging, *Carbohydr. Polym.*, 2020, **227**, 115348, DOI: 10.1016/j.carbpol.2019.115348.

18 T. Gasti, S. Dixit, O. J. D'souza, V. D. Hiremani, S. K. Vootla, S. P. Masti, R. B. Chougale and R. B. Malabadi, Smart biodegradable films based on chitosan/methylcellulose containing Phyllanthus reticulatus anthocyanin for monitoring the freshness of fish fillet, *Int. J. Biol. Macromol.*, 2021, **187**, 451–461, DOI: 10.1016/j.ijbiomac.2021.07.128.

19 J. T. Orasugh, N. R. Saha, G. Sarkar, D. Rana, R. Mishra, D. Mondal, S. K. Ghosh and D. Chattopadhyay, Synthesis of methylcellulose/cellulose nano-crystals nanocomposites: Material properties and study of sustained release of ketorolac tromethamine, *Carbohydr. Polym.*, 2018, **188**, 168–180, DOI: 10.1016/j.carbpol.2018.01.108.

20 A. Kamari and E. Phillip, Chitosan, gelatin and methylcellulose films incorporated with tannic acid for food packaging, *Int. J. Biol. Macromol.*, 2018, **120**, 1119–1126, DOI: 10.1016/j.ijbiomac.2018.08.169.

21 S. Madihalli, S. P. Masti, M. P. Eelager, R. B. Chougale, L. K. Kurabetta, A. A. Hunashyal, N. P. Dalbanjan and S. P. Kumar, Quinic acid and montmorillonite integrated chitosan/pullulan active films with potent antimicrobial and barrier properties to prolong the shelf life of tofu, *Food Biosci.*, 2024, **62**, 105492, DOI: 10.1016/j.fbio.2024.105492.

22 R. Wills and Y. Li, Use of arginine to inhibit browning on fresh cut apple and lettuce, *Postharvest Biol. Technol.*, 2016, **113**, 66–68, DOI: 10.1016/j.postharvbio.2015.11.006.

23 Z. Pakkish and S. Mohammadrezakhani, Quality characteristics and antioxidant activity of the mango (Mangifera indica) fruit under arginine treatment, *J. plant physiol. breed.*, 2021, **11**, 63–74.

24 J. Song, H. Feng, M. Wu, L. Chen, W. Xia and W. Zhang, Preparation and characterization of arginine-modified chitosan/hydroxypropyl methylcellose antibacterial film, *Int. J. Biol. Macromol.*, 2020, **145**, 750–758, DOI: 10.1016/j.ijbiomac.2019.12.141.

25 J. Cui, Y. Sun, L. Wang, Q. Miao, W. Tan and Z. Guo, Preparation of l-arginine Schiff bases modified chitosan derivatives and their antimicrobial and antioxidant properties, *Mar. Drugs*, 2022, **20**, 688, DOI: 10.3390/md20110688.

26 S. S. Narasagoudr, V. G. Hegde, R. B. Chougale, S. P. Masti, S. Vootla and R. B. Malabadi, Physico-chemical and functional properties of rutin induced chitosan/poly (vinyl alcohol) bioactive films for food packaging applications, *Food Hydrocolloids*, 2020, **109**, 106096, DOI: 10.1016/j.foodhyd.2020.106096.

27 K. S. Salem, N. K. Kasera, M. A. Rahman, H. Jameel, Y. Habibi, S. J. Eichhorn, A. D. French, L. Pal and L. A. Lucia, Comparison and assessment of methods for cellulose crystallinity determination, *Chem. Soc. Rev.*, 2023, **52**, 6417–6446, DOI: 10.1039/D2CS00569G.

28 S. Roy, J.-W. Rhim and L. Jaiswal, Bioactive agar-based functional composite film incorporated with copper sulfide nanoparticles, *Food Hydrocolloids*, 2019, **93**, 156–166, DOI: 10.1016/j.foodhyd.2019.02.034.

29 V. D. Hiremani, S. Khanapure, T. Gasti, N. Goudar, S. K. Vootla, S. P. Masti, R. B. Malabadi, B. S. Mudigoudra and R. B. Chougale, Preparation and physicochemical assessment of bioactive films based on chitosan and starchy powder of white turmeric rhizomes (Curcuma Zedoaria) for green packaging applications, *Int. J. Biol. Macromol.*, 2021, **193**, 2192–2201, DOI: 10.1016/j.ijbiomac.2021.11.050.

30 M. P. Eelager, S. P. Masti, S. Madihalli, N. Gouda, L. K. Kurbetta, M. N. Gunaki, A. A. Hunashyal and R. B. Chougale, The Effect of Cetrimide Crosslinking on Biodegradable PVA/Xanthan Gum Herbicidal Films: Towards Sustainable Agriculture and Its Influence on Soil Fertility, *J. Environ. Chem. Eng.*, 2025, **13**(2), 116029, DOI: 10.1016/j.jece.2025.116029.

31 M. S. Sarwar, M. B. K. Niazi, Z. Jahan, T. Ahmad and A. Hussain, Preparation and characterization of PVA/nanocellulose/Ag nanocomposite films for antimicrobial food packaging, *Carbohydr. Polym.*, 2018, **184**, 453–464, DOI: 10.1016/j.carbpol.2017.12.068.

32 K. S. Salem, M. Debnath, S. Agate, K. M. Y. Arafat, H. Jameel, L. Lucia and L. Pal, Development of multifunctional sustainable packaging from acetylated cellulose micro-nanofibrils (CMNF), *Carbohydr. Polym. Technol. Appl.*, 2024, **7**, 100421, DOI: 10.1016/j.carpta.2024.100421.

33 L. K. Kurabetta, S. P. Masti, M. P. Eelager, M. N. Gunaki, S. Madihalli, A. A. Hunashyal, R. B. Chougale, P. K. SK and A. J. Kadapure, Physicochemical and antioxidant properties of tannic acid crosslinked cationic starch/chitosan based active films for ladyfinger packaging application, *Int. J.*

Biol. Macromol., 2023, **253**, 127552, DOI: 10.1016/j.ijbiomac.2023.127552.

34 M. Madar, V. Srinivasan, K. R. Yamini, M. S. Pujar, M. M. Basanagouda, D. Divya and A. H. Sidarai, Miniscule modification of coumarin-based potential biomaterials: Synthesis, characterization, computational and biological studies, *J. Photochem. Photobiol., A*, 2023, **445**, 115044, DOI: 10.1016/j.jphotochem.2023.115044.

35 J. Liu, S. Liu, X. Zhang, J. Kan and C. Jin, Effect of gallic acid grafted chitosan film packaging on the postharvest quality of white button mushroom (Agaricus bisporus), *Postharvest Biol. Technol.*, 2019, **147**, 39–47, DOI: 10.1016/j.postharvbio.2018.09.004.

36 C. Wang, X. Zhang, Y. Gao, Y. Han and X. Wu, Path analysis of non-enzymatic browning in Dongbei Suancai during storage caused by different fermentation conditions, *Food Chem.*, 2021, **335**, 127620, DOI: 10.1016/j.foodchem.2020.127620.

37 M. Misenan, M. Isa and A. Khiar, Electrical and structural studies of polymer electrolyte based on chitosan/methyl cellulose blend doped with BMIMTFSI, *Mater. Res. Express*, 2018, **5**, 055304, DOI: 10.1088/2053-1591/aac25b.

38 J. Song, H. Feng, M. Wu, L. Chen, W. Xia and W. Zhang, Preparation and characterization of arginine-modified chitosan/hydroxypropyl methylcellose antibacterial film, *Int. J. Biol. Macromol.*, 2020, **145**, 750–758, DOI: 10.1016/j.ijbiomac.2019.12.141.

39 K. Wang, Z. Qi, S. Pan, S. Zheng, H. Wang, Y. Chang, H. Li, P. Xue, X. Yang and C. Fu, Preparation, characterization and evaluation of a new film based on chitosan, arginine and gold nanoparticle derivatives for wound-healing efficacy, *RSC Adv.*, 2020, **10**, 20886–20899, DOI: 10.1039/D0RA03704D.

40 M. Alizadeh-Sani, M. Tavassoli, E. Mohammadian, A. Ehsani, G. J. Khaniki, R. Priyadarshi and J.-W. Rhim, pH-responsive color indicator films based on methylcellulose/chitosan nanofiber and barberry anthocyanins for real-time monitoring of meat freshness, *Int. J. Biol. Macromol.*, 2021, **166**, 741–750, DOI: 10.1016/j.ijbiomac.2020.10.231.

41 H. H. Hefni, M. Nagy, M. M. Azab and M. H. Hussein, O-Acylation of chitosan by l-arginine to remove the heavy metals and total organic carbon (TOC) from wastewater, *Egypt. J. Pet.*, 2020, **29**, 31–38, DOI: 10.1016/j.ejpe.2019.10.001.

42 S. Huang, Y. Xiong, Y. Zou, Q. Dong, F. Ding, X. Liu and H. Li, A novel colorimetric indicator based on agar incorporated with Arnebia euchroma root extracts for monitoring fish freshness, *Food Hydrocolloids*, 2019, **90**, 198–205, DOI: 10.1016/j.foodhyd.2018.12.009.

43 T. Gasti, S. Dixit, O. J. D'souza, V. D. Hiremani, S. K. Vootla, S. P. Masti, R. B. Chougale and R. B. Malabadi, Smart biodegradable films based on chitosan/methylcellulose containing Phyllanthus reticulatus anthocyanin for monitoring the freshness of fish fillet, *Int. J. Biol. Macromol.*, 2021, **187**, 451–461, DOI: 10.1016/j.ijbiomac.2021.07.128.

44 F. Bigi, H. Haghighi, H. W. Siesler, F. Licciardello and A. Pulvirenti, Characterization of chitosan-hydroxypropyl methylcellulose blend films enriched with nettle or sage leaf extract for active food packaging applications, *Food Hydrocolloids*, 2021, **120**, 106979, DOI: 10.1016/j.foodhyd.2021.106979.

45 S. Madihalli, S. P. Masti, M. P. Eelager, R. B. Chougale, B. M. Anilkumar and A. N. Priyadarshini, Methylcellulose/Chitosan bioactive films enriched with Achyranthes aspera leaves extract: An innovative approach for sustainable cosmetic face mask applications, *Int. J. Biol. Macromol.*, 2025, **303**, 140611, DOI: 10.1016/j.ijbiomac.2025.140611.

46 S. Mukerji and T. Kar, Thermal and spectroscopic studies of as-grown L-arginine hydrochloride monohydrate crystals, *Mater. Chem. Phys.*, 1998, **57**, 72–76, DOI: 10.1016/S0254-0584(98)00169-2.

47 K. Manzoor, M. Ahmad, S. Ahmad and S. Ikram, Removal of Pb(ii) and Cd(ii) from wastewater using arginine cross-linked chitosan–carboxymethyl cellulose beads as green adsorbent, *RSC Adv.*, 2019, **9**, 7890–7902, DOI: 10.1039/C9RA00356H.

48 M. P. Eelager, S. P. Masti, N. P. Dalbanjan, S. Madihalli, M. N. Gunaki, L. K. Kurbetta, P. K. SK and R. B. Chougale, Atrazine integrated biodegradable poly (vinyl alcohol)/xanthan gum active films for mulching applications: An alternative to microplastic generation plastic mulch, *Prog. Org. Coat.*, 2024, **192**, 108510, DOI: 10.1016/j.porgcoat.2024.108510.

49 N. Goudar, V. N. Vanjeri, S. Dixit, V. Hiremani, S. Sataraddi, T. Gasti, S. K. Vootla, S. P. Masti and R. B. Chougale, Evaluation of multifunctional properties of gallic acid crosslinked Poly (vinyl alcohol)/Tragacanth Gum blend films for food packaging applications, *Int. J. Biol. Macromol.*, 2020, **158**, 139–149, DOI: 10.1016/j.ijbiomac.2020.04.223.

50 V. D. Hiremani, T. Gasti, S. P. Masti, R. B. Malabadi and R. B. Chougale, Polysaccharide-based blend films as a promising material for food packaging applications: Physicochemical properties, *Iran. Polym. J.*, 2022, **31**, 503–518, DOI: 10.1007/s13726-021-01014-8.

51 A. Abdel-Mohti, A. N. Garbash, S. Almagahwi and H. Shen, Effect of layer and film thickness and temperature on the mechanical property of micro-and nano-layered PC/PMMA films subjected to thermal aging, *Materials*, 2015, **8**, 2062–2075, DOI: 10.3390/ma8052062.

52 H. Tang, P. Zhang, T. L. Kieft, S. J. Ryan, S. M. Baker, W. P. Wiesmann and S. Rogelj, Antibacterial action of a novel functionalized chitosan-arginine against Gram-negative bacteria, *Acta Biomater.*, 2010, **6**, 2562–2571, DOI: 10.1016/j.actbio.2010.01.002.

53 S. Madihalli, S. P. Masti, M. P. Eelager, R. B. Chougale, N. P. Dalbanjan and S. K. Praveen Kumar, Sodium alginate/poly (vinyl alcohol) active films incorporated with Chrysanthemum leaves extract as an eco-friendly approach to extend the shelf life of green chilies, *Int. J. Biol. Macromol.*, 2025, **302**, 140926, DOI: 10.1016/j.ijbiomac.2025.140926.

54 H. Tang, P. Zhang, T. L. Kieft, S. J. Ryan, S. M. Baker, W. P. Wiesmann and S. Rogelj, Antibacterial action of a novel functionalized chitosan-arginine against Gram-negative bacteria, *Acta Biomater.*, 2010, **6**, 2562–2571, DOI: 10.1016/j.actbio.2010.01.002.

55 S. Roy and J.-W. Rhim, Agar-based antioxidant composite films incorporated with melanin nanoparticles, *Food Hydrocoll.*, 2019, **94**, 391–398, DOI: 10.1016/j.foodhyd.2019.03.038.

56 Z. W. Abdullah and Y. Dong, Biodegradable and water resistant poly (vinyl) alcohol (PVA)/starch (ST)/glycerol (GL)/halloysite nanotube (HNT) nanocomposite films for sustainable food packaging, *Front. Mater. Sci.*, 2019, **6**, 58, DOI: 10.3389/fmats.2019.00058.

57 R. A. Lahmer, A. P. Williams, S. Townsend, S. Baker and D. L. Jones, Antibacterial action of chitosan-arginine against Escherichia coli O157 in chicken juice, *Food Control*, 2012, **26**, 206–211, DOI: 10.1016/j.foodcont.2012.01.039.

58 J. Kumirska, M. X. Weinhold, J. Thöming and P. Stepnowski, Biomedical activity of chitin/chitosan based materials—influence of physicochemical properties apart from molecular weight and degree of N-acetylation, *Polym*, 2011, **3**, 1875–1901, DOI: 10.3390/polym3041875.

59 P. Cazón, M. Vázquez and G. Velazquez, Composite films with UV-barrier properties based on bacterial cellulose combined with chitosan and poly (vinyl alcohol): study of puncture and water interaction properties, *Biomacromolecules*, 2019, **20**, 2084–2095, DOI: 10.1021/acs.biomac.9b00317.

60 Y. Lei, L. Mao, J. Yao and H. Zhu, Improved mechanical, antibacterial and UV barrier properties of catechol-functionalized chitosan/polyvinyl alcohol biodegradable composites for active food packaging, *Carbohydr. Polym.*, 2021, **264**, 117997, DOI: 10.1016/j.carbpol.2021.117997.

61 H. Yong, X. Wang, R. Bai, Z. Miao, X. Zhang and J. Liu, Development of antioxidant and intelligent pH-sensing packaging films by incorporating purple-fleshed sweet potato extract into chitosan matrix, *Food Hydrocoll.*, 2019, **90**, 216–224, DOI: 10.1016/j.foodhyd.2018.12.015.

62 T. Gasti, S. Dixit, S. P. Sataraddi, V. D. Hiremani, S. P. Masti, R. B. Chougale and R. B. Malabadi, Physicochemical and biological evaluation of different extracts of edible Solanum nigrum L. leaves incorporated chitosan/poly (vinyl alcohol) composite films, *J. Polym. Environ.*, 2020, **28**, 2918–2930, DOI: 10.1007/s10924-020-01832-6.

63 W. Zhang, X. Li and W. Jiang, Development of antioxidant chitosan film with banana peels extract and its application as coating in maintaining the storage quality of apple, *Int. J. Biol. Macromol.*, 2020, **154**, 1205–1214, DOI: 10.1016/j.ijbiomac.2019.10.275.

64 J. Ghaderi, S. F. Hosseini, N. Keyvani and M. C. Gómez-Guillén, Polymer blending effects on the physicochemical and structural features of the chitosan/poly (vinyl alcohol)/fish gelatin ternary biodegradable films, *Food Hydrocolloids*, 2019, **95**, 122–132, DOI: 10.1016/j.foodhyd.2019.04.021.

65 R. Tanwar, V. Gupta, P. Kumar, A. Kumar, S. Singh and K. K. Gaikwad, Development and characterization of PVA-starch incorporated with coconut shell extract and sepiolite clay as an antioxidant film for active food packaging applications, *Int. J. Biol. Macromol.*, 2021, **185**, 451–461, DOI: 10.1016/j.ijbiomac.2021.06.179.

66 Y. Wu, Y. Ying, Y. Liu, H. Zhang and J. Huang, Preparation of chitosan/poly vinyl alcohol films and their inhibition of biofilm formation against Pseudomonas aeruginosa PAO1, *Int. J. Biol. Macromol.*, 2018, **118**, 2131–2137, DOI: 10.1016/j.ijbiomac.2018.07.061.

67 V. Ramji and M. Vishnuvarthanan, Chitosan ternary bio nanocomposite films incorporated with MMT K10 nanoclay and spirulina, *Silicon*, 2022, **14**, 1209–1220, DOI: 10.1007/s12633-021-01045-z.

68 V. D. Hiremani, T. Gasti, S. P. Masti, R. B. Malabadi and R. B. Chougale, Polysaccharide-based blend films as a promising material for food packaging applications: Physicochemical properties, *Iran. Polym. J.*, 2022, **31**, 503–518, DOI: 10.1007/s13726-021-01014-8.

69 M. Carissimi, S. H. Flôres and R. Rech, Effect of microalgae addition on active biodegradable starch film, *Algal Res.*, 2018, **32**, 201–209, DOI: 10.1016/j.algal.2018.04.001.

70 N. A. Jashi, M. Debnath, L. Lucia, L. Pal, M. M. Rahman and K. S. Salem, Upcycling Leather and Paper Wastes to Biodegradable Materials for Packaging Displaying Excellent Multifunctional Barrier Properties, *J. Polym. Environ.*, 2025, 1–15, DOI: 10.1007/s10924-025-03526-3, DOI: 10.1007/s10924-025-03526-3.

71 Z. Breijyeh, B. Jubeh and R. Karaman, Resistance of gram-negative bacteria to current antibacterial agents and approaches to resolve it, *Molecules*, 2020, **25**, 1340, DOI: 10.3390/molecules25061340.

72 Y. Hussein, E. M. El-Fakharany, E. A. Kamoun, S. A. Loutfy, R. Amin, T. H. Taha, S. A. Salim and M. Amer, Electrospun PVA/hyaluronic acid/L-arginine nanofibers for wound healing applications: Nanofibers optimization and *in vitro* bioevaluation, *Int. J. Biol. Macromol.*, 2020, **164**, 667–676, DOI: 10.1016/j.ijbiomac.2020.07.126.

73 M. Liang, Z. Wang, H. Li, L. Cai, J. Pan, H. He, Q. Wu, Y. Tang, J. Ma and L. Yang, l-Arginine induces antioxidant response to prevent oxidative stress *via* stimulation of glutathione synthesis and activation of Nrf2 pathway, *Food Chem. Toxicol.*, 2018, **115**, 315–328, DOI: 10.1016/j.fct.2018.03.029.

74 N. P. Dalbanjan, A. J. Kadapure and P. K. SK, A comprehensive review on latent role of stress proteins in antibiotic resistance, *The Microbe*, 2024, **4**, 100151, DOI: 10.1016/j.microb.2024.100151.

75 F. Wang, C. Xie, R. Ye, H. Tang, L. Jiang and Y. Liu, Development of active packaging with chitosan, guar gum and watermelon rind extract: Characterization, application and performance improvement mechanism, *Int. J. Biol. Macromol.*, 2023, **227**, 711–725, DOI: 10.1016/j.ijbiomac.2022.12.210.

76 S. Kumar, J. C. Boro, D. Ray, A. Mukherjee and J. Dutta, Bionanocomposite films of agar incorporated with ZnO

nanoparticles as an active packaging material for shelf life extension of green grape, *Heliyon*, 2019, 5, DOI: 10.1016/j.heliyon.2019.e01867.

77 T. T. Nguyen, T.-T. H. Nguyen, B.-T. T. Pham, T. Van Tran, L. G. Bach, P. Q. B. Thi and C. H. Thuc, Development of poly (vinyl alcohol)/agar/maltodextrin coating containing silver nanoparticles for banana (Musa acuminate) preservation, *Food Packag. Shelf Life*, 2021, **29**, 100740, DOI: 10.1016/j.fpsl.2021.100740.

78 L. Paravisini and D. G. Peterson, Mechanisms non-enzymatic browning in orange juice during storage, *Food Chem.*, 2019, **289**, 320–327, DOI: 10.1016/j.foodchem.2019.03.049.